Optical study of c-axis charge dynamics in $YBa_2Cu_3O_y$: Carrier self-confinement in the normal and the superconducting states

S. Tajima, J. Schützmann,* S. Miyamoto,† I. Terasaki, Y. Sato, and R. Hauff
Superconductivity Research Laboratory, International Superconductivity Technology Center, Shinonome 1-10-13, Koto-ku, Tokyo 135, Japan

(Received 12 December 1995; revised manuscript received 13 November 1996)

The optical conductivity spectra of $YBa_2Cu_3O_y$ crystals have been investigated with polarization $E\|c$ over a wide doping range from the heavily underdoped to the overdoped regime, focusing on the charge dynamics in the c direction. For overdoped crystals, the conductivity spectra $\sigma_c(\omega)$ show a completely metallic T and ω dependence, which can be analyzed by an extended Drude model. However, the obtained quasiparticle scattering rate γ_c is one order larger than the in-plane value, which is quite different from the case of a conventional low-dimensional material with a strong mass anisotropy. It is evidence for a non-Fermi-liquid state in high-T_c cuprates and suggests unconventional charge dynamics along the c axis such as incoherent hopping. With decreasing oxygen content y, temperature dependence of the low-ω conductivity changes from a metallic to a semiconducting one, being consistent with the T dependence of the dc resistivity ρ_c. The conductivity for the underdoped crystals with $d\rho_c(T)/dT<0$ are characterized by a suppression of the conductivity below $\omega_{\text{suppression}}(\approx 500-800\ \text{cm}^{-1})$. This doping dependence of $\sigma_c(\omega,T)$ indicates a change from a strongly confined regime for low doping to a weakly confined regime for high doping, and suggests that the mechanism of carrier confinement is closely related to strong electron correlation. The carrier-confined state which is symbolized by a large scattering rate leads to a dirty limit behavior for the c direction in the superconducting state, whereas it is in a clean limit in the plane direction. There are a couple of experimental facts which suggest a d-wave gap. A huge amount of unpaired carriers and no decrease of maximum gap amplitude were found for the overdoped crystals, which does not support the mean-field theory for explanation of the T_c drop in the overdoped regime. [S0163-1829(97)07109-9]

I. INTRODUCTION

Among many characteristic features of the high-T_c superconducting cuprates (HTSC's), one of the most attractive properties is ''a strong anisotropy'' in the electronic system. The question whether it is really two dimensional or anisotropic three dimensional has been discussed by many theorists and experimentalists. The problem is, in other words, how to treat ''anisotropy.'' If it can be described by a mass anisotropy, the system turns out to be anisotropic three dimensional, even if the mass is renormalized by a strong interaction.

A recent observation of a Josephson current in the c direction of $Bi_2Sr_2CaCu_2O_{8+z}$ (BSCCO) is strongly suggestive of a two-dimensional nature of HTSC's.[1] Our optical study of this system, indicating that the c-axis superfluid plasma frequency should be much lower than the far-infrared region, also supports a Josephson plasma picture in BSCCO.[2] However, for another typical HTSC, $YBa_2Cu_3O_y$ (YBCO) with smaller anisotropy, there is no direct observation of a Josephson current along the c axis. It should be noted that if the coherence length ξ is smaller than the interplane distance, the c axis supercurrent becomes a tunneling current through Josephson junctions. Therefore, the Josephson current along the c axis can be, in general, understood within a conventional Fermi-liquid model if one assumes a large effective mass m_c^* and a small ξ_c.

For the normal state, the semiconducting temperature dependence of the c-axis resistivity $d\rho_c/dT<0$ together with the metallic in-plane resistivity ρ_{ab} might indicate the two-dimensional nature of HTSC's, because it is the most remarkable difference from conventional low-dimensional systems. A good reference is Sr_2RuO_4 which is a recently discovered superconductor with $T_c=0.9K$.[3] Although its crystal structure is the same as that of $La_{2-x}Sr_xCuO_4$ (LSCO), a typical HTSC, and the mass anisotropy is almost the same or rather larger than LSCO, the temperature dependence of the c-axis resistivity is metallic at low temperature. In this sense, Sr_2RuO_4 is a ''strongly anisotropic three-dimensional'' material.

The origin of the semiconducting T dependence of ρ_c in HTSC's has been discussed by many research groups.[4] For some theoretical models,[5] this is crucial for high-T_c superconductivity. Recently Takenaka *et al.* reported that the characteristic temperature at which $d\rho_c/dT$ changes its sign from positive to negative scales with the spin-gap temperature and attributed this transition to the opening of a spin gap.[6] From an optical study, Homes *et al.* have found a gaplike structure around 200 cm^{-1} in the c-axis optical conductivity of $YBa_2Cu_3O_{6.7}$ well above T_c.[7] This seemed to support a spin-charge separation model in which a spin gap causes a charge gap in the c-axis conductivity.[8] However, since the spectrum has a rich structure due to phonons and/or other excitations, resulting in a complicated temperature dependence, this pseudogap problem has not been resolved yet. On the other hand, an effort to examine the low-T limit behavior of ρ_c is in progress, suppressing superconductivity by a strong magnetic field.[9] Moreover, the fact that the highly oxygenated

YBCO shows a metallic T and ω dependence[10] might throw a doubt on the argument that the diverging ρ_c in the low-T limit is essential for HTSC's.

Concerning a superconducting gap, there has been a long debate whether a superconducting gap is observable in the in-plane reflectivity spectrum or not.[11] Using the two-component model in which a spectrum is decomposed into a T-dependent Drude part and a T-independent midinfrared absorption part, Kamaras *et al.* claimed that a gap cannot be observed in the in-plane spectrum because of clean-limit superconductivity.[12] However, the origin of the midinfrared absorption is not clear, and it is questionable whether the midinfrared absorption can be regarded as an incoherent conduction channel that does not interfere with the coherent part. The other approach is based on the one-component model, which gives a gap of about 500 cm^{-1}.[13] This problem seems to be still controversial. By contrast, since there is no remarkable effect of the midinfrared absorption on the c-axis far-infrared spectrum, one could expect to observe a gap in the far-infrared spectrum, which enables us to discuss gap energy, its symmetry, its relation to T_c, etc.

For the study of the temperature dependence of the electronic c-axis conductivity, the YBCO system has the advantage, in contrast to other HTSC's such as BSCCO and LSCO, of its relatively high conductivity in the c direction. In this paper, we report on the precise temperature dependence of the c-axis optical spectrum of YBCO with various oxygen contents, focusing on the electronic properties. By subtracting phononic contributions, a systematic change in the temperature dependence of the electronic conductivity spectrum is revealed. On a basis of this result, we discuss the c-axis conduction mechanism in the normal and the superconducting states of HTSC's.

II. EXPERIMENTALS

Large single crystals were grown from the melt of $Ba_3Cu_5O_8$ and Y_2BaCuO_5 in Y_2O_3 crucibles by a modified Czochralski method. Details of the crystal growth are described in Ref. 14. A typical size of an as-grown crystal is $10\times10\times5$ mm^3, which is limited by the crucible size. Observing the x-ray Laue pattern, a crystal is cut along the c axis into several pieces with thicknesses of about 1 mm. Each piece was then annealed under different conditions in order to attain the required oxygen content.

The composition ratio and the impurity levels were analyzed by an inductively coupled plasma method. The atomic ratio of Y, Ba, and Cu was exactly 1:2:3 within a measurement error of 2–3%, indicating no impurity phase. No other element, such as Al, Ti, Mg, Sr, and Pt was detected. The composition analysis by electron-probe microanalysis also confirmed that there is no secondary phase such as Y_2BaCuO_5 and $Ba_3Cu_5O_8$.

For full oxygenation, the crystal pieces were annealed at 380–400 °C in oxygen atmosphere for 1–3 months. This annealing process gives an oxygen content $y\geq6.9$. To prepare a complete insulating crystal with $y\approx6.1$, we annealed a crystal at 600 °C in Ar atmosphere for a week. For preparation of oxygen deficient crystals with $6.1<y<6.9$, the crystal pieces were encapsulated in an evacuated quartz tube together with polycrystalline powders whose oxygen content

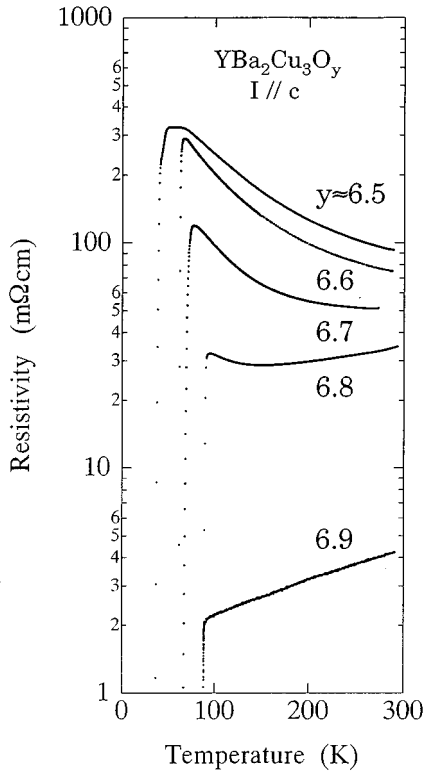

FIG. 1. Temperature dependence of the out-of-plane resistivity for $YBa_2Cu_3O_y$ with various oxygen contents y, measured by a four-probe method.

was controlled by a preceding quench process, and then annealed at 550 °C for a week. The oxygen content of the polycrystalline powders was determined by an iodometric titration analysis to be $y=6.8$, 6.7, 6.6, and 6.5. The oxygen content of each single crystal is expected to be the same as that of the polycrystals annealed in the same tube. The crystals for resistivity measurements were annealed in the same tube as the corresponding pieces for optical measurement. The ac-susceptibility measurements were performed on the same samples used in the optical study.

The superconducting transition temperature T_c was determined by the ac-susceptibility and the dc-resistivity measurements. The details of the transport properties such as resistivity, Hall coefficient, Seebeck coefficient are reported in a separate paper.[15] Owing to our large crystal size, the resistivity measurement by the four-probe method can be carried out not only in the *ab* but also in the c direction. Figure 1 shows the temperature dependence of the out-of-plane (c-axis) resistivity for various oxygen contents y. These results are in good agreement with those reported by Ito *et al.*[16] As the oxygen content decreases, the resistivity increases dramatically. Only for $y\approx6.9$, the c-axis resistivity exhibits a complete metallic temperature dependence down to T_c of 88 K which is slightly lower than T_c of 92 K for $y\approx6.8$.[17] The low resistivity and the low T_c in the crystal with $y\approx6.9$ strongly suggest an overdoped state of this crystal.[17] Other evidence for overdoping for $y\approx6.9$ was reported in Refs. 15 and 18 in detail. The c-axis resistivity for optimal doping ($y\approx6.8$) decreases with decreasing temperature and shows a slight upturn close to T_c. For all the other y, ρ_c increases when the temperature approaches T_c. To confirm the homo-

geneity of oxygen content, we have also measured the acsusceptibility of the crystals for all oxygen contents. It was found that the superconducting transition is sharp in all the crystals ($\Delta T_c = 0.5$ K for $y \approx 6.9$ and 2 K for $y \approx 6.6$), indicating homogeneous oxygen distribution within the crystals.

All superconducting crystals show a fine twin structure. The average domain size is about 10 μm in the *ab* direction and 100 μm in the *c* direction, which was observed using an optical polarized microscope. The ac faces, large enough for an accurate measurement of far-infrared spectra, were polished by Al_2O_3 powder with a size of 0.3 μm, prior to the optical measurement.

The optical reflectivity spectra were measured using a Fourier transformation-type infrared spectrometer and a He-gas flow cryostat in the wave number region from 30 to 9000 cm^{-1} and a grating-type spectrometer in the range from 4000 to 30 000 cm^{-1}. The reflected light was polarized along the *c* axis by wire grid polarizers on polyethylene substrate for $\omega = 30-300$ cm^{-1} and on KRS-5 substrate for $\omega = 250-4000$ cm^{-1} as well as a quartz polarizer for $\omega > 4000$ cm^{-1}. The incident light was focused on the sample surfaces with a spot diameter of about 2 mm. The reflectivity intensity was compared to that reflected from a Au-evaporated mirror, which was precisely replaced for the sample at each temperature. The angles of the sample and the mirror surface were aligned relative to the optical path by using a He-Ne laser during measurement. By evacuating the cryostat and the spectrometer simultaneously, we could use thin polyethylene film 30 μm as cryostat windows in the far-infrared range. Owing to the thin window, we could get high signals and see the focus of the visible part of the radiation on the sample. The latter advantage enabled us to readjust the sample position after cooling, which is necessary because with reducing temperature the sample holder shrinks and consequently the focus moves on the sample surface. In this way, the reproducibility of reflectivity measurement is excellent, and the accuracy in the reflectivity better than 1%.

III. RESULTS AND ANALYSIS

A. Reflectivity spectra

Figure 2 shows the c-axis room-temperature reflectivity spectra of $YBa_2Cu_3O_y$ for various y. For $y \approx 6.1$, five phonon peaks which are predicted for the tetragonal D_{4h}^1 symmetry by group theory are clearly observed. The electronic contribution is negligible. As the oxygen content increases, free carrier contribution increases, resulting in an increase of the average far-infrared reflectivity. For the highly oxygenated crystal with $y \approx 6.9$, the reflectivity is very high in the far-infrared region and a clear plasma minimum is observed around 2000 cm^{-1}. Five small peaks due to phonon absorptions are superposed on this plasma spectrum, which is consistent with the group-theoretical analysis for the orthorhombic D_{2h}^1 symmetry, except for the missing Ba-vibrational phonon at the lowest frequency that might be screened by the free carriers. With reducing the oxygen content, another phonon peak grows around 630 cm^{-1}, while the peak at 570 cm^{-1} loses its strength. Both are associated with the apical oxygen vibrational mode, which is strongly affected by the oxygen coordination of the Cu(1) chain site.[19]

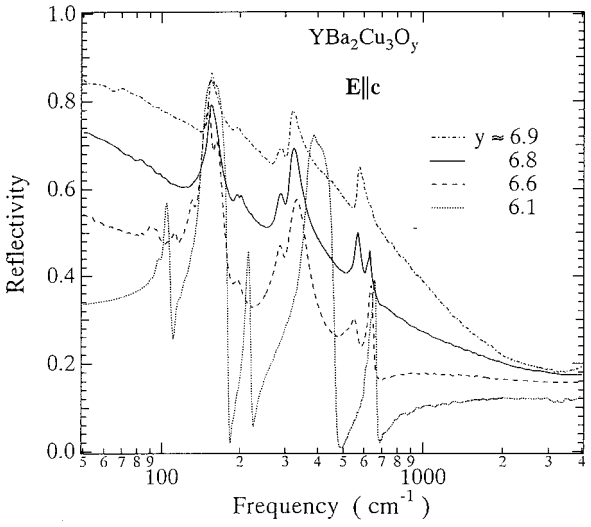

FIG. 2. The room-temperature reflectivity spectra of $YBa_2Cu_3O_y$ with $E \| c$ for various y.

The systematic low-ω spectral growth with increasing y was reported in detail for room temperature by Cooper *et al.*[20] Our results have confirmed it in a wider doping range from almost nondoped insulator to the metal in the overdoped regime. This low-ω spectral growth with doping is observed also in LSCO (Ref. 21) and thus probably common feature in the c-axis spectrum of the high-T_c materials. As reported in Ref. 20 and also seen in Fig. 2, the spectral growth below 0.5 eV in the c-axis spectrum is slower than that in the in-plane spectrum. This seems to imply that, in addition to the strong correlation effect which disturbs the itinerancy of carriers in the low doping regime, the c-axis charge conduction is strongly disturbed even in the high doping regime.

The c-axis reflectivity spectra at 10 K are shown in Fig. 3 for various y in comparison with the normal state spectra at 100 K. More precise temperature dependence of the reflectivity spectra were reported in our previous paper.[19] For $y \approx 6.9$ an appreciable temperature dependence is observed up to high frequency around 2000 cm^{-1}. With reducing y, the temperature-dependent spectral region becomes limited to the far-infrared region. In the spectrum for $y \approx 6.9$, the low-ω reflectivity increases remarkably below T_c, while it decreases between 400 and 800 cm^{-1}, forming an edge structure around 300 cm^{-1}. For $y \approx 6.8$, this edge shifts to about 200 cm^{-1}, and for $y \approx 6.6$, lower than 100 cm^{-1}. Usually an edge-like feature is associated with the opening of a superconducting gap. In dirty limit, the frequency below which the reflectivity R is exactly equal to 1.0 corresponds to a superconducting gap energy 2Δ, while in the case of a d-wave or gapless superconductor, the edge structure due to deviation from $R = 1.0$ is smeared out. On the other hand, a sharp reflectivity edge must not necessarily indicate a gap energy. For a special case, if the screened plasma energy for superconducting carriers is smaller than the gap energy, it represents a collective excitation of the superfluid plasma. This was typically observed in the c-axis spectrum of LSCO,[22] where the screened plasma frequency of superconducting carriers, corresponding to the zero-crossing frequency in $\epsilon_1(\omega)$, lies below a superconducting gap. The

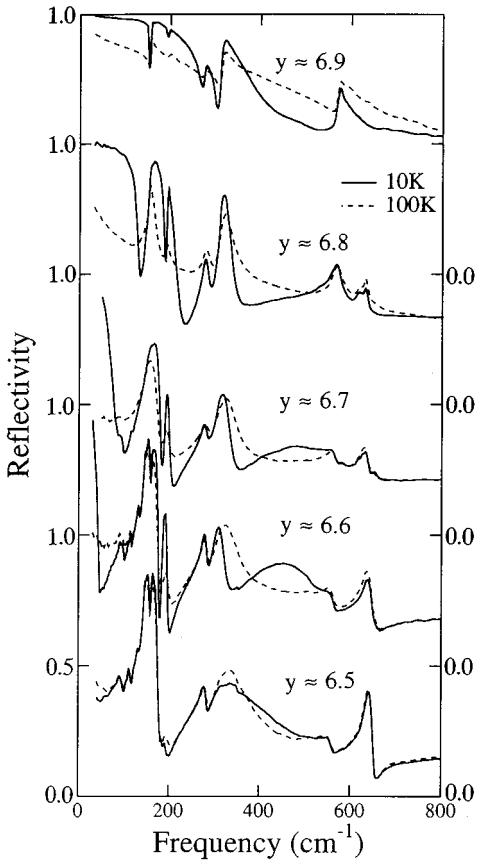

FIG. 3. Doping dependence of the c-axis reflectivity spectra of $YBa_2Cu_3O_y$ in the superconducting state (10 K) in comparison with the normal state spectra at 100 K.

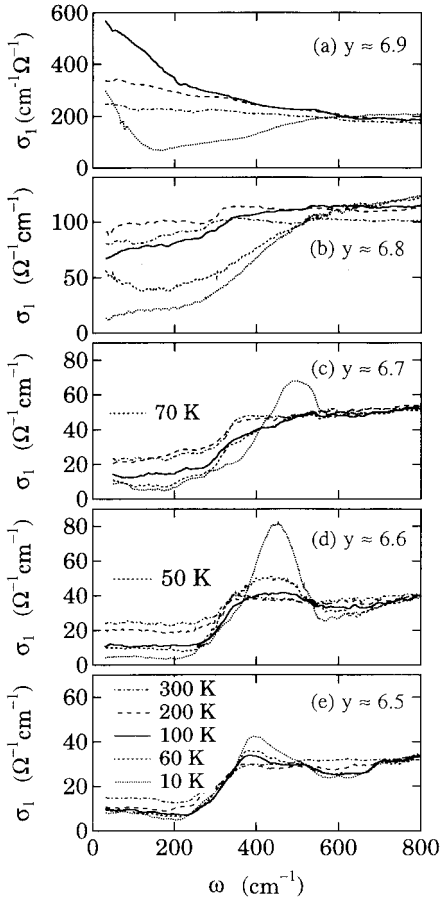

FIG. 4. Temperature dependence of the c-axis optical conductivity spectra of $YBa_2Cu_3O_y$ for $y \approx 6.9$ (a), 6.8 (b), 6.7 (c), 6.6 (d), and 6.5 (e), in which the phonon contributions are subtracted by fitting based on the modified Lorentz oscillator model.

spectrum for $y \approx 6.6$ in Fig. 3 is similar to the spectrum of $La_{1.85}Sr_{0.15}CuO_4$,[22] suggesting the latter special case, and then the shift of the edge with doping indicates an increase in the superconducting carrier density. When the plasma edge energy exceeds the gap energy, the reflectivity threshold should turn out to be responsible for a superconducting gap as in a conventional case with $\hbar\omega_p > 2\Delta$. This crossover is observed between $y \approx 6.8$ and 6.9, which can be confirmed by the conductivity spectra shown in the next subsection.

In addition to the appearance of a sharp edge, there is another dramatic change around 500 cm^{-1} for the underdoped crystals. It is linked with the phonon anomaly for the in-plane oxygen bending mode.[19,23]

B. Conductivity spectra

A Kramers-Kronig analysis for the reflectivity data was performed to obtain the conductivity spectra. For the high-frequency extrapolation, reflectivity above 4 eV (32 000 cm^{-1}) is assumed to be constant up to 10 eV and to decrease as ω^{-4} above it. For low frequencies, the reflectivity spectra were extrapolated using a Drude formula above T_c and a two-fluid model below T_c. We have tried several extrapolation and checked their effects on the results.

Figures 4 and 5 show the real part of the complex conductivity spectra and the real part of the dielectric function of YBCO for various oxygen contents, corresponding to the data in Figs. 2 and 3. In Fig. 4, sharp peaks due to the phonon absorptions are subtracted by fitting to obtain the electronic conductivity spectra. The conductivity spectra including phonon contributions as well as the fitting procedure are described in detail in Ref. 19. For the overdoped crystal, phonon peaks are almost symmetric and can be well fitted with conventional Lorentz oscillators. However, with decreasing oxygen content, some phonon peaks show asymmetric line shapes. Thus, a modified Lorentz oscillator model with asymmetric parameter was used for fitting. After subtraction of all sharp phonon resonances, a broad peak around 450 cm^{-1} remains. Although it grows as a result of spectral weight transfer from the in-plane oxygen bending mode at 320 cm^{-1}, suggesting a phononic origin of this peak, the peak profile is so broad that a further decomposition of the spectra in a proper way is impossible. As the oxygen content decreases, the low frequency conductivity at $\omega \to 0$ decreases, which is consistent with the doping dependence of the dc resistivity shown in Fig. 1. In Fig. 5, one can see a systematic shift of the zero-crossing frequency in the dielectric function $\epsilon_1(\omega)$ at 10 K, which causes the sharp reflectivity edge below T_c. In the underdoped regime, at this zero-crossing frequency, one can see a sharp reflectivity edge but no distinct structure in the conductivity spectrum in Fig. 4, which confirms that this reflectivity edge does not correspond to a superconducting gap but to a plasma edge for the superconducting carriers. In the overdoped crystal for

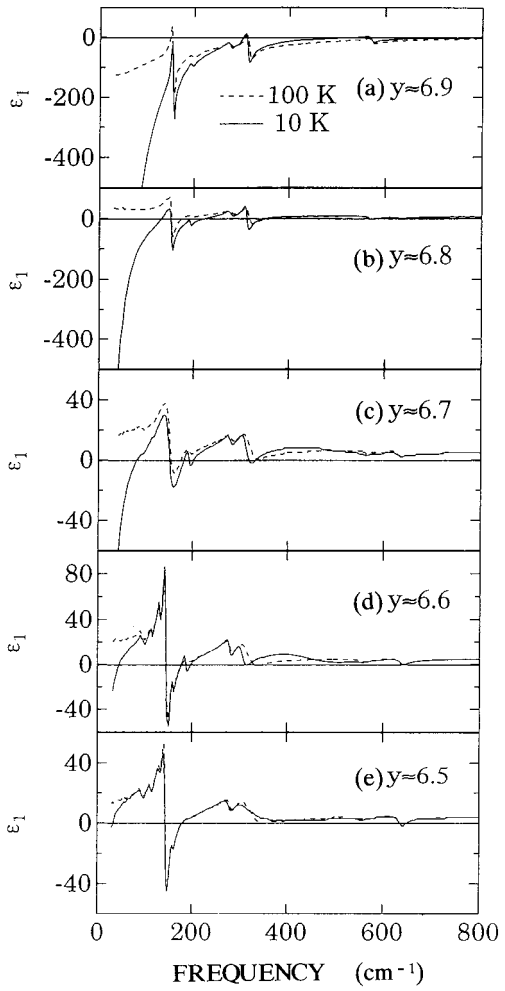

FIG. 5. Temperature dependence of the real part of the dielectric function $\epsilon_1(\omega)$ of $YBa_2Cu_3O_y$ for $y\approx 6.9$ (a), 6.8 (b), 6.7 (c), 6.6 (d), and 6.5 (e), which were calculated from the reflectivity spectra in Fig. 4 by a Kramers-Kronig analysis.

$y\approx 6.9$, the frequency at which a pronounced reflectivity drop is observed below T_c roughly corresponds to the threshold frequency for the conductivity decrease, indicating that the appearance of a reflectivity edge is due to an opening of a gap.

The room-temperature conductivity for $y\approx 6.9$ is about 250 Ω^{-1} cm^{-1} at $\omega\rightarrow 0$ and it becomes more than 600 Ω^{-1} cm^{-1} at 100 K. This is the highest σ_c value of YBCO reported so far, implying the high doping level of this crystal. With decreasing temperature, the low-ω conductivity increases, forming a Drude-like curve. The metallic temperature dependence of the far-infrared conductivity is consistent with the dc resistivity behavior in Fig. 1. Below T_c the conductivity is strongly suppressed at $\omega<650$ cm^{-1}, as a result of the spectral weight transfer to a δ function at $\omega=0$. The threshold frequency of about 650 cm^{-1}, therefore, seems to correspond to a superconducting gap energy. However, even at 10 K, well below T_c, there remains a pronounced conductivity at low frequencies, suggesting a gapless superconductivity. The Drude-like conductivity increase below 200 cm^{-1} suggests the existence of unpaired carriers in the superconducting state. This upturn of conductivity was observed also in the other overdoped YBCO crystals (not shown in this paper), and disappears in the optimally doped crystal with $y\approx 6.8$, that is, this phenomenon is dependent on the doping.[18] The spectra of overdoped LSCO also show a similar behavior.[24]

The normal-state spectrum for $y\approx 6.8$ is almost flat and less temperature dependent. When the temperature decreases from 300 down to 200 K, σ_1 increases over a wide frequency range, which can be understood as a result of reduction of plasma damping, although it is a highly damped plasmon. Then, when the temperature further decreases, σ_1 decreases only below 500 cm^{-1}. This σ_1 decrease at low frequencies proceeds also below T_c, forming a gaplike structure with a long tail. The temperature dependence of σ_1 at $\omega\rightarrow 0$ is in good agreement with the dc resistivity behavior in Fig. 1, which shows the sign change in $d\rho/dT$ between 200 and 100 K. As mentioned above, the spectral behavior above 200 K can be understood as a change of plasma damping. However, the low-ω suppression below 200 K strongly suggests a different mechanism, governing the temperature dependence of the c-axis conductivity.

The σ_1 suppression at low ω from far above T_c is commonly observed in the underdoped crystals. For $y=6.7$, 6.6, and 6.5, the conductivity below 250 cm^{-1} is almost flat and monotonously decreases with decreasing temperature. The conductivity above 800 cm^{-1} is almost temperature independent. A complicated and dramatic temperature dependence of the spectrum is seen for intermediate frequencies. Ignoring the spectral growth around 400 cm^{-1}, a clear σ_1 suppression is observed below 700 cm^{-1} in our data for $y\approx 6.6$ and 6.5, which disagrees with the phonon subtracted spectra reported by Homes *et al.*[25] The growth of a new peak around 400 cm^{-1} makes it difficult to identify a gap structure. Although a monotonous decrease of low ω-conductivity below 200 cm^{-1} below T_c indicates an opening of a gap, a finite conductivity is clearly observed at the lowest temperature.

IV. DISCUSSION

A. Normal state

In discussion about the conduction mechanism along the c axis, the metallic T dependence of ρ_c in the well-oxygenated YBCO has often been referred to. Since T_c for the most anisotropic material, BSCCO with a semiconductorlike ρ_c, is almost the same as that for the least anisotropic material, YBCO with a metallic ρ_c, dimensionality seems to have no relation to the high-T_c superconductivity. Sometimes, in the theoretical model which stresses the interlayer hopping for the c-axis conduction mechanism,[26] fully oxygenated YBCO is regarded as an exception. On the other hand, for the theoretical model which insists on a metallic conduction in the c direction, YBCO is a preferable compound.[27] Therefore, it is of great importance to examine whether YBCO can be regarded as an anisotropic three-dimensional metal or not, in other words, whether the anisotropy can be described by a large mass anisotropy or not.

The first approach is to analyze the conductivity spectrum on the assumption of the metallic regime. The most typical metallic behavior of the c-axis conductivity is observed in the overdoped YBCO with $y\approx 6.9$. Only at this composition

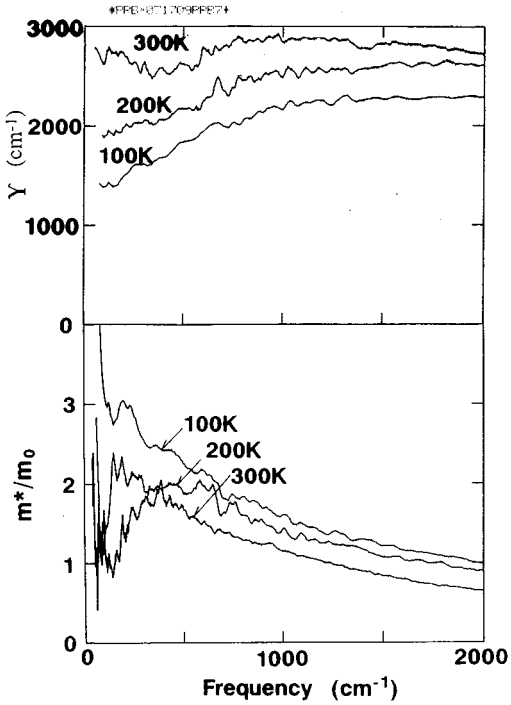

FIG. 6. Temperature dependence of the effective mass $m^*(\omega)$ and the scattering rate $1/\tau(\omega)=\gamma(\omega)$ for $y\approx 6.9$, which were calculated from the phonon-subtracted complex conductivity based on an extended Drude model.

the plasmon is well defined at room temperature, that is, ϵ_1 crosses zero above the highest phonon frequency. Subtracting the phonon peaks and the midinfrared absorption by a Lorentz oscillator fit, we obtain the electronic conductivity spectra which can be analyzed by an extended Drude model as follows:

$$\epsilon(\omega)=\epsilon_\infty-\frac{\omega_p^{*2}(\omega)}{\omega^2+i\omega\gamma^*(\omega)}, \tag{1}$$

$$\omega_p^{*2}(\omega)=\frac{4\pi ne^2}{m^*(\omega)}. \tag{2}$$

Here the frequency dependences of the effective mass $m^*(\omega)=m[1+\lambda(\omega)]$ and the scattering rate $\gamma^*(\omega)=\gamma(\omega)m/m^*(\omega)$ originate from the coupling of carriers with some optically inactive excitation via the coupling constant $\lambda(\omega)$. In Fig. 6, $m^*(\omega)$ and $\gamma(\omega)$ are shown, calculated from the complex conductivity spectrum in Figs. 4(a) and 5(a). First, one realizes that the strong temperature dependence of ρ_c is mainly caused by a strong temperature dependence of γ_c, not by that of m_c^*. (The data scattering in m_c^* below 400 cm^{-1} are due to imperfect subtraction of the phonon contributions. The extrapolation of the high-frequency curve gives more reliable value of m_c^* at $\omega\rightarrow 0$.) Second, the value of γ_c is extremely large. Using the reported values for ω_{pa} and γ_a in the a direction,[13] the anisotropy ratio of the dc resistivity ($\rho_c/\rho_a\approx 40-100$) can be roughly explained by the multiplication of the mass ratio $[(\omega_{pa}/\omega_{pc})^2\approx 7]$ and the scattering rate ratio ($\gamma_c/\gamma_a\approx 10$). Note that the mass ratio of 7 is in good agreement with the band calculation.[28] This implies that a strong anisotropic resistivity originates not only from the mass anisotropy, but also from the scattering rate anisotropy. In a conventional Fermi-liquid metal the real-space anisotropy in the scattering rate is not strong. Therefore, the difference of an order of magnitude in the scattering rate indicates a completely different scattering mechanism between the in-plane and the out-of plane directions. The origin of this large γ_c must be related with an incoherent conduction mechanism, which is more typically seen in BSCCO (Ref. 2) and LSCO.[29,24] In this sense, even overdoped YBCO with the least anisotropy cannot be regarded as an anisotropic three-dimensional metal but rather as a two-dimensional system. In fact, the mean-free path l_c ($\sim$5.8 Å), which was estimated from γ_c ($\sim$2800 cm^{-1}) and ω_{pc} ($\sim$5700 cm^{-1}),[15] is shorter than the interlayer spacing ($\sim$11 Å). This implies that the c-axis conduction is not coherent.

It may be worthwhile to compare HTSC's with the recently discovered superconductor Sr_2RuO_4 (Ref. 3) that is isostructural to LSCO. Owing to its layered structure, the anisotropy in the resistivity is of the same order as in LSCO. The most remarkable difference from HTSC's is the metallic temperature dependence of ρ_c at low temperature. Correspondingly, in the c-axis reflectivity spectrum, a sharp plasma edge appears in the normal state,[30] indicating a small scattering rate at low temperature. From this viewpoint, this system seems to be a strongly anisotropic three-dimensional Fermi liquid. In contrast, the peculiarity of HTSC's is unusual anisotropy which is not given by an anisotropic effective mass alone, but rather governed by the anisotropic scattering mechanism.

The next problem is the semiconducting temperature dependence of the c-axis conductivity, which is observed in oxygen deficient YBCO and most other HTSC's. Ignoring the steplike structure at 250 cm^{-1}, which has no T and y dependence,[23] and the broad peak growing around 400 cm^{-1} at low temperature,[19,25] we find in Fig. 4 that the normal-state conductivity is suppressed far beyond 250 cm^{-1} for all of the underdoped crystals. According to the spin-charge separation model in which the spinon-holon recombination governs the c-axis conduction, the c-axis conductivity is expected to be suppressed below a critical frequency when a gap opens in a spin excitation spectrum.[8] In this scenario, the crossover temperature $T_{\rm cross}$, at which $d\rho_c/dT$ changes its sign, should correspond to the spin gap temperature $T_{\rm spin}$ ($\approx$120 K).[31] However, the observed $T_{\rm cross}$ is far above $T_{\rm spin}$ and is rather close to T^* ($\approx$400 K) which is the critical temperature for reduction of the uniform susceptibility.[32] Moreover, if we compare the critical frequency for this conductivity suppression $\omega_{\rm suppression}$ 500–800 cm^{-1}) with the spin gap energy $\hbar\omega_{\rm spin}$(=32 meV) determined by the neutron-scattering measurement,[33] it is found that $\omega_{\rm suppression}$ is much higher than $\omega_{\rm spin}$.

Another possible approach is based on the following phenomenological expressions:

$$\rho_c=C_1\rho_a+C_2/T \tag{3}$$

or

$$\rho_c=C_1\rho_a+C_2\exp(\Delta_c/kT). \tag{4}$$

The former expression was proposed for the Luttinger-liquid interlayer hopping by Anderson and Zou[5] and the latter is an experimentally deduced model by Ong and co-workers.[34] In our previous paper,[15] we examined several models to analyze the c-axis resistivity data for the overdoped crystal, and found that the metallic T dependence can be well fitted to the above formula. The terms in series for the resistivity mean that there are two scattering mechanisms. The first term in Eqs. (4) and (5) arises from the in-plane scattering and the second represents the interplane hopping that is an origin of the non-Fermi-liquid behavior in the c-axis charge dynamics. Since it is not a parallel conduction but a series, a complicated spectral behavior is expected, in other words, it is difficult to extract only one of these two contributions from the observed spectrum. However, we can discuss the limiting cases that either the first or the second term dominates ρ_c. In the former case, the conductivity spectrum is metallic, while in the latter it becomes a semiconductorlike spectrum.

Returning to our experimental data, the spectrum for the overdoped crystal [Fig. 4(a)] seems to represent the former case. Therefore, we could tentatively analyze the conductivity by an extended Drude model. Here, a contribution of the second term manifests itself in a large γ_c. On the other hand, for the underdoped crystals, the contribution of the first term is much weaker as in the latter case. The ω dependence of the second term contribution depends on the model. In case of the model for Eq. (4), the conductivity between Luttinger liquids in the resonating valence bond state is predicted to behave as $\sigma_c(\omega) \sim \omega^{4\alpha}$, α being the Luttinger-liquid exponent.[26] On the other hand, for the model which predicts a charge gap in the c direction[8] a gaplike structure should be observed in the conductivity. Even if such a gap has a s-wave symmetry, a small contribution of the first term could smear the gap structure, causing a gradual reduction of the conductivity with decreasing frequency. An even more complicated behavior is expected for a gap with d-wave symmetry. The localization picture which also gives a similar σ_1 suppression at low frequencies is unlikely, because it is incompatible to the completely metallic spectrum in the a direction for the same material. Whatever the model for the second term is, the above concept of a series of resistivity implying the existence of two scattering mechanisms is necessary to explain the spectral change with doping and temperature. As a result of combination of the two terms, the critical frequency for σ_1 suppression changes with doping, depending on the admixing of the first term, even if the gap energy Δ_c is constant. Therefore, the observed tendency that the conductivity suppression becomes more pronounced with reducing y, as seen in Fig. 4, can be understood by the increase in the second term contribution and/or the increase in the gap Δ_c with reducing y.

B. Superconducting state

In the in-plane spectrum, observation of a superconducting gap has been a hotly disputed issue. One of the opinions is that the quasiparticle scattering rate is so small that it is difficult to observe a gap structure, implying clean limit superconductivity.[12] In contrast, in the c direction it is clear that the system is in a dirty limit because the obtained γ_c ($\sim$1000 cm^{-1}) is larger than the possible gap frequency ($\hbar\gamma_c \gg 2\Delta$), which is equivalent to the relation $l \ll \xi_0$. When the plasma frequency decreases with reducing doping level, it becomes harder to determine the scattering rate. Note that appearance of a sharp reflectivity edge is not an indication of the strong suppression of γ_c below T_c. The combination of a large gap 2Δ and a large γ_c could give a sharp reflectivity edge, as recently demonstrated by Kim *et al.*[29]

Although a gaplike conductivity suppression is observed below T_c in Figs. 4(a) and 4(b), the spectral profile at the lowest temperature does not look like a conventional s-wave superconductor with a clear cutoff [$\sigma(\omega)=0$] but shows a long tail. The threshold frequency, which might correspond to the maximum gap frequency $2\Delta_{\max}$ of an anisotropic gap, is about 600 cm^{-1} for $y \approx 6.8$ and 650 cm^{-1} for $y \approx 6.9$.[35] In the underdoped crystals with $y \leqslant 6.7$, it is difficult to determine the threshold frequency for a superconducting gap, because the conductivity is suppressed from the higher frequency $\omega_{\text{suppression}}$ even above T_c. What we can deduce from Fig. 4 is that $2\Delta_{\max} \leqslant \omega_{\text{suppression}}$. Furthermore, there remains ω-independent finite conductivity even at the lowest temperature. It turns out that a clear gap as well as its doping dependence is not observable in the underdoped region. Instead, we observe, in the reflectivity spectra (Fig. 3), a decrease of Josephson plasma frequency with reducing y, which could be caused by a decrease in the superconducting plasma frequency or the interlayer tunneling probability. One should notice in Fig. 4 that in spite of a lower T_c for overdoping than for optimum doping, $2\Delta_{\max}$ is slightly larger for $y \approx 6.9$ than for $y \approx 6.8$, that is, a gap energy does not scale with T_c in the overdoped region. This suggests that the T_c drop in the overdoped regime cannot be explained by the mean-field theory but is rather caused by a kind of pair breaking. Further evidence for pair breaking is a huge amount of residual conductivity forming a Drude-like increase toward $\omega=0$ [Fig. 4(a)], which was discussed in detail in our previous paper.[18]

In order to argue the c-axis conduction in the superconducting state, we have estimated the London penetration depth λ from the missing area A in the conductivity spectrum below T_c as follows.

$$\lambda_c^{-2} = A\,\delta(\omega) = \frac{8}{c^2}\int_0^{\infty} (\sigma_1^n - \sigma_1^s)\,d\omega. \tag{5}$$

In the case of clean limit superconductors, we can estimate the anisotropic ratio from the ratio λ_c^2/λ_a^2 which gives m_c^*/m_a^*. However, comparing our estimation of $\lambda_c \approx 12\,000$ Å for $y \approx 6.9$ with the reported in-plane value $\lambda_a \approx 1500$ Å, we obtain the ratio $\lambda_c^2/\lambda_a^2 \approx 64$ which is much larger than the mass ratio estimated from the plasma frequency ratio $\omega_{pa}^2/\omega_{pc}^2 \approx 7$. This is a strong support for dirty limit superconductivity in the c direction, because for a dirty superconductor only a part of the Drude weight for $\hbar\omega < 2\Delta$ condensates into a δ function at $\omega=0$. It follows that the penetration depth ratio estimated from the missing area is not equal to the plasma frequency ratio in the normal state. This peculiar feature, clean limit in the ab direction and dirty limit in the c direction, can be explained by the model in which clean-limit superconducting layers couple weakly with each other and form an array. According to this model, the supercurrent along the array direction flows

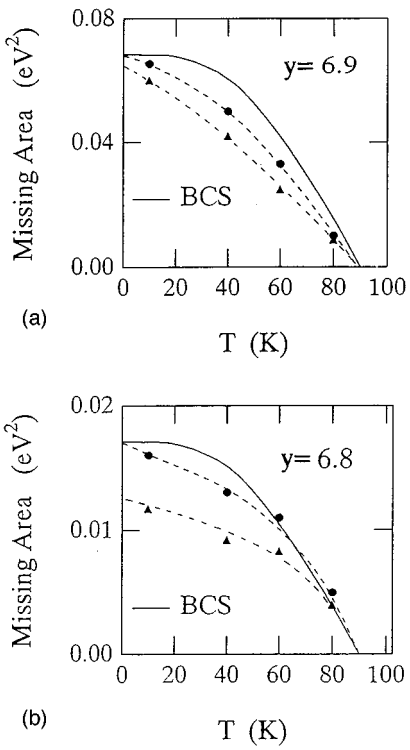

FIG. 7. Temperature dependence of the missing area in $\sigma_1(\omega)$ below 600 cm^{-1} (solid circle) and 2000 cm^{-1} (solid triangle) for $YBa_2Cu_3O_y$ with $y\approx 6.9$ (a) and 6.8 (b), which is proportional to $\lambda^2(0)/\lambda^2(T)$. The solid curve is the expectation from the BCS theory for the case of 600 cm^{-1}.

through Josephson junctions and behaves as in the dirty limit.[36] Another prediction of this model is the relation $\sigma_n \propto \lambda^{-2}$. Recently Basov *et al.* demonstrated that the relation $\sigma_c \propto \lambda_c^{-2}$ roughly holds among many of the HTSC's, assuming a constant gap energy Δ.[37]

This intrinsic Josephson coupling in one direction could occur in highly anisotropic materials where the interplane spacing d is larger than the coherence length ξ. For example, also in the organic superconductor κ-(BEDT-TTF)$_2$Cu[N(CN)$_2$]Br where the anisotropy ratio is of the order of 100, the condition $\xi < d$ is satisfied.[38] Therefore, the c-axis Josephson current can be understood within a Fermi-liquid picture and is not the direct evidence for unconventional charge transport along the c axis. However, the confinement of the quasiparticles is also observable in the superconducting state. Although it is difficult to determine the scattering rate of the quasiparticles below T_c, the fact that the superconductivity is in dirty limit for the c direction ($l_c \ll \xi_c$) and in clean limit for the a direction ($\xi_a \ll l_a$) with anisotropic coherence lengths ($\xi_c < \xi_a$), implies that mean-free paths are strongly anisotropic ($l_c \ll l_a$). Furthermore, as is mentioned below, the missing area estimated below 2000 cm^{-1} is smaller than that estimated below 600 cm^{-1} (Fig. 7). This indicates that the confined state which is piled up to the high-ω spectral region does not move back to the low-ω coherent state even below T_c.

Finally we discuss the gap symmetry. It is often referred to the temperature dependence of the penetration depth. In Fig. 7, we plot the temperature dependence of the missing area in the conductivity spectra for $y\approx 6.8$ and 6.9, which is proportional to $\lambda_c^{-2}(T)$. The problem for estimation of λ_c is the cutoff frequency for integration in Eq. (6). As seen in Fig. 4, the lowest temperature spectrum crosses the normal state spectrum for 100 K around 600 cm^{-1}. In the frequency range between 600 and 2000 cm^{-1} the conductivity at 6 K is a little larger than that at 100 K, while it is T independent above 2000 cm^{-1}. This means that the missing spectral weight below T_c is not completely transferred to a δ function at $\omega = 0$ but partly to a higher frequency range. Therefore, the penetration depth estimated from the missing area below 2000 cm^{-1} is larger than that estimated from the area below 600 cm^{-1}. Both for $y\approx 6.8$ and 6.9, the temperature dependences of λ_c are different from the normal BCS behavior. The missing area, i.e., $\lambda_c^2(0)/\lambda_c^2(T)$ increases more linearly with reducing temperature than in the BCS case, which is preferable for an anisotropic superconductivity with nodes in a gap, being consistent with the results of the microwave measurement.[39]

Although it is difficult to conclude the gap symmetry from the optical measurements, there are a couple of observations in the present work which suggest a strongly anisotropic superconducting gap. The first is the conductivity spectral profile at $T \ll T_c$ showing a tail towards $\omega = 0$, which indicates a finite absorption at $\omega \to 0$. This spectral profile is in good agreement with the theoretical prediction for a d-wave symmetry by Graf *et al.*[40] The second is the fact that a finite density of states appears at E_F very easily owing to some kind of pair breaking. Besides the present result of the overdoping effect, our preliminary measurement on the Zn-substituted YBCO (Ref. 41) indicated a strong absorption within the gap. It is consistent with the results of the other techniques which revealed a finite density of states at E_F owing to pair breaking by impurities such as Zn.[42] The third is the temperature dependence of the penetration depth mentioned just above. From all these results, a strongly anisotropic gap is more plausible than an isotropic s wave.

V. CONCLUSION

The optical reflectivity spectra of $YBa_2Cu_3O_y$ single crystals were measured for the polarization with $E \| c$ over wide doping, temperature, and frequency ranges. The large sizes of our crystals enabled us to determine the reflectivity with high accuracy in the far-infrared region. By subtracting the phonon contributions, we successfully extracted the electronic components of the conductivity spectra $\sigma_c(\omega)$ for $YBa_2Cu_3O_y$ with various y, which reveal a unique electronic state in HTSC's that is characterized by ''the carrier confinement'' both in the normal and superconducting states.

The non-Fermi-liquid state called ''carrier confinement'' manifests itself in a large anisotropy in the carrier scattering rate $1/\tau$ for the overdoped YBCO and in the c-axis conductivity suppression below 500–800 cm^{-1} for the underdoped YBCO, which is in strong contrast to a Fermi-liquid metal. Assuming a two scattering mechanism, i.e., series resistivity for the conventional Boltzmann scattering and the incoherent interlayer hopping, and taking into account of their doping dependence, we can understand the whole doping and T dependence of the c-axis conductivity spectrum.

This carrier confinement regime seems to be maintained even below T_c. An appearance of a sharp edge in the

c-axis reflectivity spectrum below T_c does not imply a rapid decrease in the quasiparticle scattering rate, but is simply an indication that $\hbar\omega'_{ps}<2\Delta$. The dirty limit behavior evidenced by a large penetration depth ratio λ_c^2/λ_a^2 together with the clean limit in the plane direction, implies a large anisotropy in the mean-free path, i.e., an anisotropy in $1/\tau$. Moreover, the conductivity spectral weight pushed above 600 cm^{-1} due to the confinement in the normal state does not seem to condense into a δ function at $\omega=0$.

For highly oxygenated crystals a superconducting gaplike feature is clearly observed in the c-axis optical spectra. There are a couple of observations suggesting a strongly anisotropic gap. In the overdoped regime, the maximum gap amplitude does not decrease in spite of the T_c suppression. This, together with an increase of the residual unpaired carriers at $T\ll T_c$, indicates a peculiar pair-breaking mechanism causing a decrease of T_c in the overdoped regime.

ACKNOWLEDGMENTS

The authors are indebted to Y. Yamada and Y. Shiohara at Superconductivity Research Laboratory for the crystal growth of $YBa_2Cu_3O_y$. They thank S. Uchida at the University of Tokyo for useful discussion. This work was partially supported by NEDO for R&D of Industrial Science and Technology Frontier Program.

*Present address: Solid State Physics Laboratory, University of Groningen, Nijenborgh 4, Groningen, The Netherlands.

†Present address: Toshiba Battery Co., Technology Research Laboratory, Shinagawa-ku, Minami-shinagawa 3-4-10, Tokyo 140, Japan.

[1] R. Kleiner, F. Steinmeyer, G. Kunkel, and P. Müller, Phys. Rev. Lett. **68**, 2394 (1992).

[2] S. Tajima, G. D. Gu, S. Miyamoto, A. Odagawa, and N. Koshizuka, Phys. Rev. B **48**, 16 164 (1993).

[3] Y. Maeno, H. Hashimoto, K. Yoshida, S. Nishizaki, T. Fujita, J. G. Bednorz, and F. Lichtenberg, Nature (London) **372**, 532 (1994).

[4] For a review, S. L. Cooper and K. E. Gray, in *Physical Properties of the High Temperature Superconductors IV*, edited by D. M. Ginsberg (World Scientific, Singapore, 1994), p. 61, and references therein.

[5] P. W. Anderson and Z. Zou, Phys. Rev. Lett. **60**, 132 (1988); P. W. Anderson, *ibid.* **67**, 3844 (1991).

[6] K. Takenaka, K. Mizuhashi, H. Takagi, and S. Uchida, Phys. Rev. B **50**, 6534 (1994).

[7] C. C. Homes, T. Timusk, R. Liang, D. A. Bonn, and W. N. Hardy, Phys. Rev. Lett. **71**, 1645 (1993).

[8] N. Nagaosa, J. Phys. Chem. Solids **53**, 1493 (1992).

[9] Y. Ando, G. S. Boebinger, A. Passner, T. Kimura, and K. Kishio, Phys. Rev. Lett. **75**, 4662 (1995).

[10] J. Schützmann, S. Tajima, S. Miyamoto, and S. Tanaka, Phys. Rev. Lett. **73**, 174 (1994).

[11] For a review, D. B. Tanner and T. Timusk, in *Physical Properties of High Temperature Superconductors III*, edited by D. M. Ginsberg (World Scientific, Singapore, 1992), and references therein.

[12] K. Kamaras, S. L. Herr, C. D. Porter, N. Tache, D. B. Tanner, S. Etemad, T. Venkatesan, E. Chase, A. Inam, X. D. Wu, M. S. Hedge, and B. Dutta, Phys. Rev. Lett. **64**, 84 (1990).

[13] Z. Schlesinger, R. T. Collins, F. Holtzberg, C. Feild, S. H. Blanton, U. Welp, G. W. Crabtree, Y. Fang, and J. Z. Liu, Phys. Rev. Lett. **65**, 801 (1990).

[14] Y. Yamada and Y. Shiohara, Physica C **217**, 182 (1993).

[15] I. Terasaki, Y. Sato, S. Miyamoto, S. Tajima, and S. Tanaka, Phys. Rev. B **52**, 16 246 (1995).

[16] T. Ito, K. Takenaka, and S. Uchida, Phys. Rev. Lett. **70**, 3995 (1993).

[17] We determined the y value by the iodometric titration for the corresponding polycrystals. The obtained values are smaller than those expected from the dc resistivity, compared with the reported values. However, the precise absolute value of y is not so important here.

[18] J. Schützmann, S. Tajima, S. Miyamoto, Y. Sato, and I. Terasaki, Solid State Commun. **94**, 293 (1995).

[19] J. Schützmann, S. Tajima, S. Miyamoto, Y. Sato, and R. Hauff, Phys. Rev. B **52**, 13 665 (1995).

[20] S. L. Cooper, D. Reznik, A. Kotz, M. A. Karlow, R. Liu, M. V. Klein, W. C. Lee, J. Giapintzakis, D. M. Ginsberg, B. W. Veal, and A. P. Paulikas, Phys. Rev. B **47**, 8233 (1993); P. Nyhus, M. A. Karlow, S. L. Cooper, B. W. Veal, and A. P. Paulikas, *ibid.* **50**, 13 898 (1994).

[21] K. Tamasaku, T. Ito, H. Takagi, and S. Uchida, Phys. Rev. Lett. **72**, 3088 (1994).

[22] K. Tamasaku, Y. Nakamura, and S. Uchida, Phys. Rev. Lett. **69**, 1455 (1992).

[23] S. Tajima, J. Schützmann, and S. Miyamoto, Solid State Commun. **95**, 759 (1995).

[24] S. Uchida, K. Tamasaku, and S. Tajima, Phys. Rev. B **53**, 14 558 (1996).

[25] C. C. Homes, T. Timusk, D. A. Bonn, R. Liang, and W. N. Hardy, Physica C **254**, 265 (1995).

[26] D. G. Clarke, S. P. Strong, and P. W. Anderson, Phys. Rev. Lett. **74**, 4499 (1995).

[27] N. Kummar and A. M. Jayannavar, Phys. Rev. B **45**, 5001 (1992).

[28] P. B. Allen and W. E. Pickett, Phys. Rev. B **37**, 7482 (1988).

[29] J. H. Kim, H. S. Somal, M. T. Czyzyk, D. van der Marel, A. Wittlin, A. M. Gerrits, V. H. M. Duijn, N. T. Hien, and A. A. Menovsky, Physica C **247**, 297 (1995).

[30] T. Katsufuji, M. Kasai, and Y. Tokura, Phys. Rev. Lett. **76**, 126 (1996).

[31] H. Yasuoka, T. Imai, and T. Shimizu, in *Strong Correlation and Superconductivity*, edited by H. Fukuyama, S. Maekawa, and A. P. Malozemoff, Springer Series in Solid State Sciences Vol. 89 (Springer-Verlag, Berlin, 1989), p. 254; W. W. Warren, Jr., R. E. Walstedt, G. F. Brennert, R. J. Cava, R. Tycko, R. F. Bell, and G. Dabbagh, Phys. Rev. Lett. **62**, 1193 (1989).

[32] H. Alloul, T. Ohno, and P. Mendels, Phys. Rev. Lett. **63**, 1700 (1989); M. Takigawa, A. P. Reyes, P. C. Hammel, J. D. Thompson, R. H. Heffner, Z. Fisk, and K. C. Ott, Phys. Rev. B **43**, 247 (1991).

[33] J. Rossat-Mignod, L. P. Regnault, C. Vettier, P. Bourges, P. Burlet, J. Bossy, J. Y. Henry, and G. Lapertot, Physica C **185-189**, 86 (1991).

[34] N. P. Ong, Physica C **235-240**, 221 (1994); Y. F. Yan, J. M. Harris, and N. P. Ong, *ibid.* **235-240**, 1527 (1994).

[35] In our previous publication (Ref. 10), we inferred a gap energy of 300 cm^{-1} from the absoption threshold in the spectrum for $y\approx 6.9$, which is a conventional way to assign a gap energy. However, it is very hard to consider the whole of our data for a conventional s-wave superconductor. Therefore, in the present

paper we argue only a maximum gap energy which is defined by a threshold frequency for σ_1 suppression.

[36] J. R. Clem, Physica C **162–164**, 1137 (1989).

[37] D. N. Basov, T. Timusk, B. Dabroski, and J. D. Jorgensen, Phys. Rev. B **50**, 3511 (1994).

[38] W. N. Kwok, U. Welp, K. D. Carlson, G. W. Crabtree, K. G. Vandervoort, H. H. Wang, A. M. Kini, J. M. Williams, D. L. Stupka, L. K. Montgomery, and J. E. Thompson, Phys. Rev. B **42**, 8686 (1990).

[39] W. N. Hardy, D. A. Bonn, D. C. Mogan, R. Liang, and K. Zhang, Phys. Rev. Lett. **70**, 3999 (1993).

[40] M. J. Graf, M. Palumbo, D. Rainer, and J. A. Sauls, Phys. Rev. B **52**, 10 588 (1995).

[41] R. Hauff, S. Tajima, W.-J. Jang, and Y. Sato, *Advances in Superconductivity VIII* (Springer-Verlag, Berlin, in press); S. Tajima, R. Hauff, and E.-J. Jang, in *Spectroscopic Studies of Superconductors*, Proc SPIE **2696**, 25 (1996).

[42] In NMR, J.-T. Kim, T. R. Lemberger, S. R. Foltyn, and X. Wu, Phys. Rev. B **49**, 15 970 (1994); K. Ishida, Y. Kitaoka, N. Ogata, T. Kamino, K. Asayama, J. R. Cooper, and N. Athanassopoulou, J. Phys. Soc. Jpn. **62**, 2803 (1993); in specific heat, J. W. Loram, K. A. Mirza, and P. F. Freeman, Physica C **171**, 243 (1990).